Plasmonic effects for light concentration in organic photovoltaic thin films induced by hexagonal periodic metallic nanospheres

Jinfeng Zhu,[1,2,a)] Mei Xue,[1] Huajun Shen,[1] Zhe Wu,[2] Seongku Kim,[1] Jyh-Jier Ho,[1] Aram Hassani-Afshar,[1] Baoqing Zeng,[2] and Kang L. Wang[1]
[1]*Department of Electrical Engineering, University of California, Los Angeles, California 90095, USA*
[2]*School of Physical Electronics, University of Electronic Science and Technology of China, Chengdu 610054, China*

(Received 6 January 2011; accepted 23 March 2011; published online 14 April 2011)

We present a plasmonic nanostructure design by embedding a layer of hexagonal periodic metallic nanospheres between the active layer and transparent anode for bulk heterojunction organic solar cells. The hybrid structure shows broadband optical absorption enhancement from localized surface plasmon resonance with a weak dependence on polarization of incident light. We also theoretically study the optimization of the design to enhance the absorption up to 1.90 times for a typical hybrid active layer based on a low band gap material. © *2011 American Institute of Physics*. [doi:10.1063/1.3577611]

Organic photovoltaic (OPV) cell is a promising alternative to conventional silicon solar cell due to its flexibility, light weight and low cost.[1–4] However, its energy conversion efficiency is low because the light absorption depth is much larger than the exciton diffusion length in organic semiconductors.[2] Although the use of bulk heterojunction blend for OPVs partially lessens the problem of a short diffusion length of excitons before dissociation in optically thick films,[3] the use of thinner films with adequate optical absorption attracts lots of attentions for better exciton dissociation. There have been plentiful efforts in overcoming weak absorption of optically thin film of organic solar cells through using particle plasmons.[5–8] However, a systematic modeling design of the related nanostructures is much in need to optimize the enhanced optical absorption of plasmonic OPVs.

In this letter, we use a three-dimensional (3D) modeling design of a monolayer of hexagonal periodic silver nanospheres in bulk heterojunction blends to boost OPV performance through enhanced optical absorption. The structures can be practically built with some low-cost nanofabrication methods.[9] Our simulations show this nanostructure produces broadband optical absorption enhancement with a weak dependence on polarization of incident light, and the absorption enhancement originates from the light concentration by localized surface plasmon resonance (LSPR).

Our design of the plasmonic OPV is illustrated in Fig. 1. The monolayer of nanospheres is adhered to the transparent anode poly(3,4-ethylenedioxythiophene):poly(styrenesulfonate) (PEDOT:PSS) and embedded in the bulk heterojunction blend. The nanospheres and bulk heterojunction blend constitute a hybrid active layer. Metallic particles with diameters of 5–20 nm and their dielectric function dependence on the particle size are used.[10,11] Two popular bulk heterojunction blends poly(3-hexylthiophene):[6,6]-phenyl-C_{61}-butyric acid methyl ester (P3HT:PC_{60}BM, 1:1 in weight) and poly[2,6-(4,4-bis-(2-ethylhexyl)-4H-cyclopenta[2,1-b;3,4-b′] dithiophene)-alt-4,7-(2,1,3-benzothiadiazole)]:[6,6]-phenyl-C_{71}-butyric acid methyl ester (PCPDTBT:PC_{70}BM, 1:3 in weight) are compared.[12,13] P3HT:PC_{60}BM is a blue and green light absorber and PCPDTBT:PC_{70}BM is a low band gap material. All refractive media are assumed to be isotropic. We perform our simulation with a 3D finite-difference time-domain method.[14] Periodic boundary conditions and electromagnetic symmetries are assumed due to the hexagonal nanosphere periodicity, and perfectly matched layers are used to simulate optical open boundary conditions. Both *p*- and *s*-polarized light are normally incident on the anode surface.

We consider the general effect of metallic nanospheres on optical absorption in such structures and focus on the investigation in a 40 nm thick active layer considering the tradeoff of using the bulk heterojunction versus optically thin films. Normalized optical absorption spectra of pristine and hybrid active layers are shown in Fig. 2(a). The absorption spectra in hybrid active layers show enhancement compared

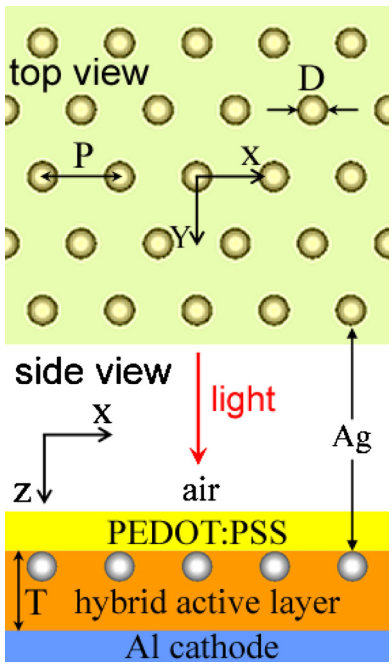

FIG. 1. (Color online) Schematic structure of the simulated plasmonic OPV cell. The symbols, T, D, and P, are active layer thickness, nanosphere diameter, and period, respectively.

a)Electronic mail: jfzhu@ucla.edu.

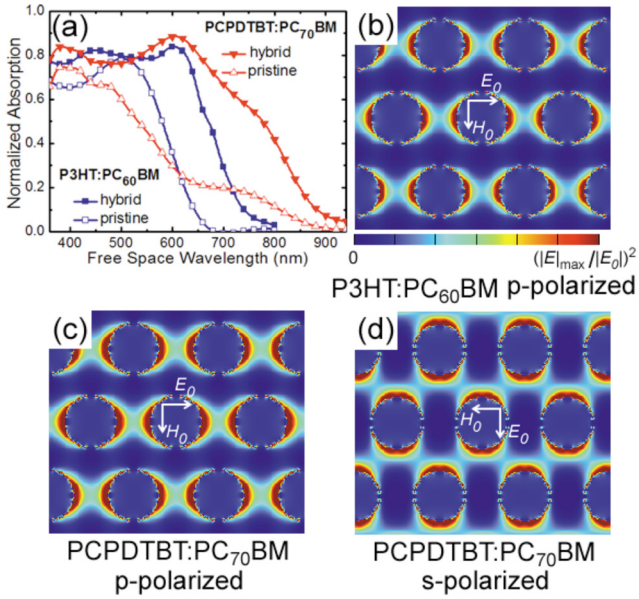

FIG. 2. (Color online) For T=40 nm, D=15 nm, and P=25 nm, (a) *p*-polarized incident absorption spectra of the pristine and hybrid active layers using P3HT:PC_{60}BM and PCPDTBT:PC_{70}BM; electric field distributions of x-y cross sections cutting through a nanosphere in hybrid active layers at λ=604 nm, (b) and (c) for *p*-polarized incidence in P3HT:PC_{60}BM and PCPDTBT:PC_{70}BM, (d) for *s*-polarized incidence in PCPDTBT:PC_{70}BM. In the color bar, E_0 and H_0 are the electric and magnetic fields of incident light source and $(|E|_{max}/|E_0|)^2$ is the normalized electric field intensity.

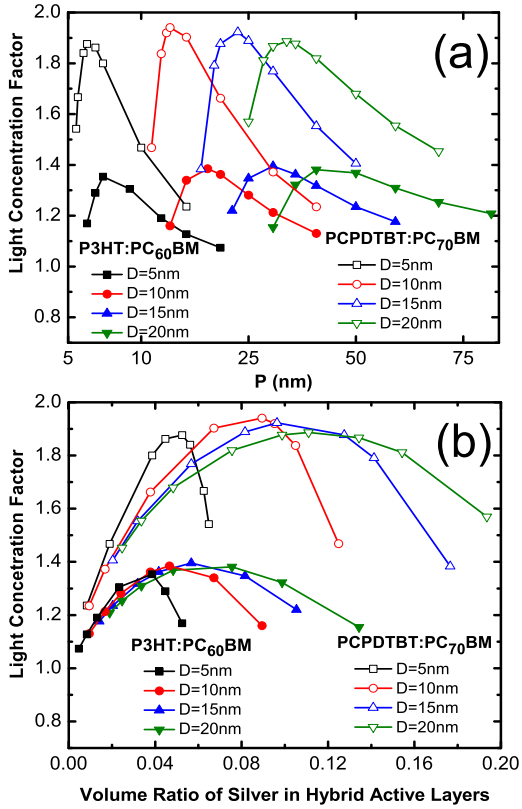

FIG. 3. (Color online) For D=5, 10, 15, and 20 nm and T=40 nm in P3HT:PC_{60}BM and PCPDTBT:PC_{70}BM, (a) Light concentration factor as a function of nanosphere period P, (b) Light concentration factor as a function of volume ratio of silver in hybrid active layers.

to the spectra of pristine active layers in the absorption bands of 360 nm–650 nm and 360 nm–900 nm for P3HT:PC_{60}BM and PCPDTBT:PC_{70}BM, respectively. The enhanced absorption peaks induced by the nanospheres are observed at about the wavelength 604 nm for both blends. Particularly, the absorption enhancement near 604 nm in the low band gap material PCPDTBT:PC_{70}BM significantly compensates the low optical absorption of the pristine active layer in the longer wavelength range. The enhanced optical absorption is due to the near-field enhancement in bulk heterojunction blends. As is known, the optical absorption in active layer materials can be calculated by $2\omega \times n \times k \int_V |E|^2 dV'$, where n and k are real and imaginary parts of material refractive index, respectively, E is the local electric field and V is the volume of material. By looking at the distributions of electric field E shown in Figs. 2(b) and 2(c), we notice strong near-field enhancement in the blends surrounding metallic nanospheres due to LSPR. The enhanced field is concentrated between nanospheres along the direction of light polarization. Both *p*- and *s*-polarized lights have their distinct electric field distributions shown in Figs. 2(c) and 2(d) but their absorption spectra are almost the same (not shown here). The above mentioned result is due to the electromagnetic symmetry of hexagonal nanosphere lattices, unlike the wire and strip nanostructures,[15,16] where the absorption spectra of *p*- and *s*-polarized lights are different. Furthermore, in the absorption bands of bulk heterojunction, most of the enhanced optical absorption takes place in the lossy blends without significant ohmic loss in metallic nanospheres, and the result is consistent with a recent study.[17] So here we only discuss spectra of *p*-polarized light and neglect the influence of loss in metallic nanospheres.

Next, effects of particle size and period on the optical absorption enhancement are also investigated. By tuning nanosphere sizes and periods, the LSPR peak locations can be engineered to optimize the total optical absorption of hybrid active layers.[11] We define the light concentration factor for hybrid active layers as

$$F = \frac{\int_{\lambda_{min}}^{\lambda_{max}} S_{hybrid}(\lambda) S_{AM1.5}(\lambda) d\lambda}{\int_{\lambda_{min}}^{\lambda_{max}} S_{pristine}(\lambda) S_{AM1.5}(\lambda) d\lambda},$$

where $\lambda_{min} \sim \lambda_{max}$ denotes the absorption band. $S_{hybrid}(\lambda)$ and $S_{pristine}(\lambda)$ are absorption spectra of hybrid and pristine active layers, respectively. $S_{AM1.5}(\lambda)$ is air mass 1.5 solar irradiance spectrum. We show the light concentration factor as a function of nanosphere diameter and period in Fig. 3(a). It further demonstrates the near-field enhancing effect of metallic nanospheres. When the particle period is much larger than the particle size, the concentration factor is reduced to 1.0. Because the evanescent field scattered by one particle is so weak in the vicinity of distant particles compared to the exciting field, the electromagnetic interactions between particles can be neglected. As the particle period decreases, the concentration factor becomes larger until it reaches the maximum at an optimum period, where the scattering field gets much larger and the particles are electromagnetically coupled.[18] The maximum factor of PCPDTBT:PC_{70}BM is around 1.90, much larger than 1.36 of P3HT:PC_{60}BM due to the LSPR spectrum enhancement in longer wavelengths. As the particle period becomes smaller than the optimum period, the factor sharply drops because of the heavy reduction in bulk heterojunction absorber volume fraction. Additionally, the factor peak shifts to larger particle spacings for increasing diameter lengths, as a result of increasing scatter-

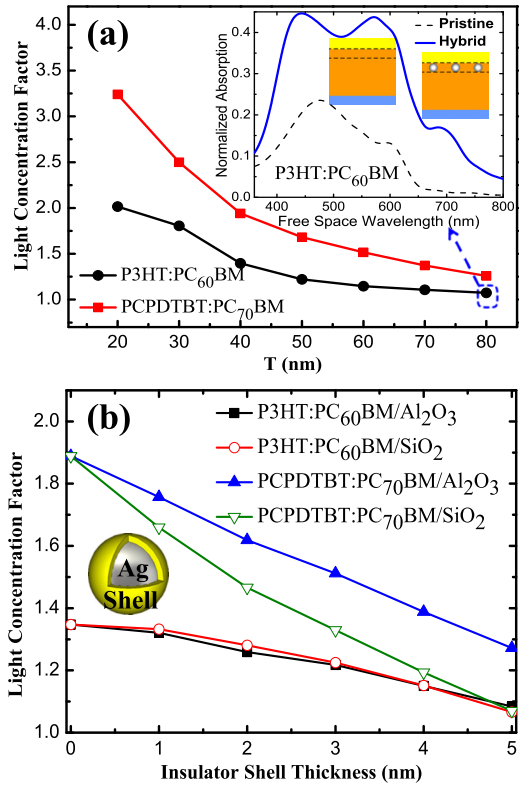

FIG. 4. (Color online) (a) Light concentration factor as a function of active layer thickness T; D=15 nm and P=30 nm for P3HT:$PC_{60}BM$; D=10 nm and P=13 nm for PCPDTBT:$PC_{70}BM$. The inset is the normalized absorption of the top 15 nm region of pristine and hybrid active layers, for T=80 nm in P3HT:$PC_{60}BM$. (b) Light concentration factor as a function of insulator shell thickness of SiO_2 and Al_2O_3, for T=40 nm, D=15 nm, and P=25 nm.

ing cross section with particle sizes.[11] In Fig. 3(b), the concentration factor peak of PCPDTBT:$PC_{70}BM$ shifts to larger volume ratio of silver (smaller periods) compared with P3HT:$PC_{60}BM$ under the same particle diameter, implying that PCPDTBT:$PC_{70}BM$ requires a higher particle density for optimum absorption enhancement.

We also consider influences of active layer thickness on optical absorption of this nanostructure. It is shown in Fig. 4(a), as the thickness decreases from 80 to 20 nm, the concentration factor increases rapidly. For 20 nm thick PCPDTBT:$PC_{70}BM$ hybrid active layer, a concentration factor as high as 3.24 is obtained. For a thicker hybrid active layer, e.g., P3HT:$PC_{60}BM$ 80 nm, there is insignificant change in total absorption but the absorption in the top 15 nm thick region of hybrid active layers is much larger than that in pristine ones due to LSPR as shown in the inset of Fig. 4(a). Excitons in active layers are redistributed and concentrated in this region of the film. The hole mobility is usually far less than the electron mobility in P3HT:$PC_{60}BM$,[19] and holes statistically reach the electrode interface slower and harder than electrons. The light energy redistribution and concentration could reduce the transport path of localized holes to the PEDOT:PSS electrode, thereby increasing device photocurrents.[6]

Finally, the optical absorption enhancement by using nanospheres with insulator shells is investigated. In some cases, exciton recombination caused by exposed metallic nanospheres in practical devices might significantly weaken the conversion efficiency improved by LSPR, so these spheres can be isolated from the bulk heterojunction blend by thin transparent insulator shells. Transparent shells with various refractive indices and thicknesses also alter LSPR peak locations.[20] Figure 4(b) illustrates the light concentration factor as a function of shell thickness using two common insulators, SiO_2 and Al_2O_3 ($n_{SiO_2}=1.46$ and $n_{Al_2O_3}=1.76$). The concentration factor reduces as the thickness increases. The reduction is more severe for SiO_2 than Al_2O_3 in the PCPDTBT:$PC_{70}BM$ hybrid active layer. This is because the refractive indices $n_{SiO_2} < n_{Al_2O_3} < n_{PCPDTBT:PC_{70}BM}$ and both shells lead to LSPR blueshifts while the shift to the short-wavelength for SiO_2 is larger than Al_2O_3 due to the smaller index. The factor can still keep as high as 1.76 when applying 1 nm Al_2O_3 shells in PCPDTBT:$PC_{70}BM$. For P3HT:$PC_{60}BM$ with a higher absorption coefficient, there is no prominent distinction on concentration factors for two kinds of shells.

In summary, we proposed the incorporation of hexagonal periodic metallic nanospheres in the OPV cells. We observed a broadband optical absorption enhancement with a weak dependence on polarization of incident light. Our systematic modeling results yielded the light concentration optimization of metallic nanosphere sizes and periods. We also investigated the influences of active layer thickness and nanosphere insulator shell on optical absorption. This letter provides a guide for the optical design of using plasmon effects to improve the absorption of organic solar cells.

The authors acknowledge the support from the joint KACST/California Center of Excellence on Nano Science and Engineering for Green and Clean Technologies.

[1]G. Li, V. Shrotriya, J. Huang, Y. Yao, T. Moriarty, K. Emery, and Y. Yang, Nature Mater. **4**, 864 (2005).
[2]S. Günes, H. Neugebauer, and N. S. Sariciftci, Chem. Rev. **107**, 1324 (2007).
[3]J. Y. Kim, K. Lee, N. E. Coates, D. Moses, T. Nguyen, M. Dante, and A. J. Heeger, Science **317**, 222 (2007).
[4]J. R. Tumbleston, D. Ko, E. T. Samulski, and R. Lopez, Appl. Phys. Lett. **94**, 043305 (2009).
[5]H. Atwater and A. Polman, Nature Mater. **9**, 205 (2010).
[6]W. Yoon, K. Jung, J. Liu, T. Duraisamy, R. Revur, F. L. Teixeira, S. Sengupta, and P. R. Berger, Sol. Energy Mater. Sol. Cells **94**, 128 (2010).
[7]A. P. Kulkarni, K. M. Noone, K. Munechika, S. R. Guyer, and D. S. Ginger, Nano Lett. **10**, 1501 (2010).
[8]K. Topp, H. Borchert, F. Johnen, A. V. Tunc, M. Knipper, E. von Hauff, J. Parisi, and K. Al-Shamery, J. Phys. Chem. A **114**, 3981 (2010).
[9]A. J. Hong, C. C. Liu, Y. Wang, J. Kim, F. Xiu, S. Ji, J. Zou, P. F. Nealey, and K. L. Wang, Nano Lett. **10**, 224 (2010).
[10]E. D. Palik, *Handbook of Optical Constants of Solids* (Academic, New York, 1985).
[11]U. Kreibig and M. Vollmer, *Optical Properties of Metal Clusters* (Springer, Berlin, 1995).
[12]G. Dennler, K. Forberich, T. Ameri, C. Waldauf, P. Denk, C. J. Brabec, K. Hingerl, and A. J. Heeger, J. Appl. Phys. **102**, 123109 (2007).
[13]F. Monestier, J.-J. Simon, P. Torchio, L. Escoubas, F. Flory, S. Bailly, R. de Bettignies, S. Guillerez, and C. Defranoux, Sol. Energy Mater. Sol. Cells **91**, 405 (2007).
[14]Lumerical FDTD Solutions, www.lumerical.com.
[15]C. Min, J. Li, G. Veronis, J. Lee, S. Fan, and P. Peumans, Appl. Phys. Lett. **96**, 133302 (2010).
[16]H. Shen, P. Bienstman, and B. Maes, J. Appl. Phys. **106**, 073109 (2009).
[17]J. Lee and P. Peumans, Opt. Express **18**, 10078 (2010).
[18]L. Gunnarsson, E. J. Bjerneld, H. Xu, S. Petronis, B. Kasemo, and M. Käll, Appl. Phys. Lett. **78**, 802 (2001).
[19]V. D. Mihailetchi, H. Xie, B. de Boer, L. J. A. Koster, and P. W. M. Blom, Adv. Funct. Mater. **16**, 699 (2006).
[20]H. Xu and M. Käll, Sens. Actuators B **87**, 244 (2002).